

# **Supporting Information**

## **Revisiting the Corrosion of Aluminum Current Collector in Lithium-Ion Batteries**

*Tianyuan Ma<sup>1,2</sup>, Guiliang Xu<sup>1</sup>, Yan Li<sup>1</sup>, Li Wang<sup>3</sup>, Xiangming He<sup>3</sup>, Jianming Zheng<sup>4</sup>, Jun Liu<sup>4</sup>, Mark H. Engelhard<sup>5</sup>, Peter Zapol<sup>6</sup>, Larry A. Curtiss<sup>6</sup>, Jacob Jorne<sup>2,7\*</sup>, Khalil Amine<sup>1</sup>, and Zonghai Chen<sup>1\*</sup>*

- 1) Chemical Sciences and Engineering Division, Argonne National Laboratory, 9700 South Cass Avenue, Lemont, IL 60439, USA
- 2) Materials Science Program, University of Rochester, Rochester, NY 14627, USA
- 3) Institute of Nuclear and New Energy Technology, Tsinghua University, Beijing 100084, China
- 4) Energy and Environmental Directorate, Pacific Northwest National Laboratory, 902 Battelle Boulevard, Richland, Washington 99354, United States
- 5) Environmental Molecular Sciences Laboratory, Pacific Northwest National Laboratory, 902 Battelle Boulevard, Richland, Washington 99354, United States
- 6) Material Science Division, Argonne National Laboratory, 9700 South Cass Avenue, Lemont, IL 60439, USA

7) Department of Chemical Engineering, University of Rochester, Rochester, NY  
14627, USA

Corresponding author: [Jacob.jorne@rochester.edu](mailto:Jacob.jorne@rochester.edu); [Zonghai.chen@anl.gov](mailto:Zonghai.chen@anl.gov)

## Tables of Contents

### Name

#### Experimental and Computational Details

Figure S1 Typical decay of current being held at certain potential for 10 hours.

Table S1 Reaction energies and oxidation potentials of EC in the presence of different functional groups on alumina calculated using B3LYP functionals and PCM solvation model.

Figure S2 Structure of EC at different state, alumina models (Alumina, Alumina1H and Alumina2H) represented by clusters derived from a periodic model of amorphous alumina.

Figure S3 Potential-dependent of the static parasitic current for conditioned aluminum foil by repeated cycling between 3.4 V and 4.9 V for 5 cycles. The electrolyte used was 1.2 M LiPF<sub>6</sub> in EC/EMC (3:7 by weight).

Figure S4 (a) XPS profiles of aluminum foils before and after the anodic treatment in 1.2 M LiFSI in EC/EMC (3:7 by weight); XPS depth profile analysis of aluminum foils (b) bare Al foil, (c) being anodic treated at 3.9 V, and (d) being anodic treated at 4.8 V.

Figure S5 Decay of current for (a) Al, (b) carbon coated Al, (c) graphene coated Al, and (d) AlPO<sub>4</sub> coated Al in LiFSI based electrolyte at 4.2 V.

Figure S6 Potential-dependent of the static parasitic current for aluminum foil in (a) 1.2 M LiPF<sub>6</sub> in FEC/EMC (3:7 by volume), (b) 1.2 M LiPF<sub>6</sub> in mixture solvent of FEC and fluorinated ether (3:7 by weight).

## Experimental and Computational Details

*Materials investigated* - Battery grade Al foil with thickness of 19  $\mu\text{m}$  was investigated. The Al foil was punched into 1.5  $\text{cm}^2$  discs and subsequently put in 75°C vacuum oven overnight. The dry Al foil was then transferred into glovebox for further use. The carbon coated Al foil (ShenZhen Perfect Power Technology Co., Ltd., 10.30.2014) and graphene coated Al foil (Ningbo Morsh Tech.Co., Ltd, GC-foil) are used without any further treatment, except for the vacuum drying overnight. The aluminum phosphate coated Al foil is home-made by washing commercial Al foil with ethanol, and then dipping the Al foil into  $\text{AlPO}_4$  solution with concentration of 2 wt.% for a certain period of time till the foil losses the metal shining and shows light white in color. Finally, the as-prepared Al foil was dried at 150 °C for about 6h.

*Electrochemical measurement* - The Al corrosion behavior in electrolyte containing 1.2 M  $\text{LiPF}_6$  in a mixture solvent of Ethylene Carbonate and Ethyl Methyl Carbonate with EC/EMC 3:7 by weight (GenII) and 1.2 M Lithium bis(fluorosulfonyl)imide ( $\text{LiFSI}$ ) in the same solvent was tested with a home-build high-precision electrochemical measurement system, which can provide high resolution data allowing the measurement of small currents for side reactions without significantly changing operation condition. Al was used as the working electrode, metallic Li foil was used as the counter electrode and Celgard 2325 was used as the separator for assembling 2032 type coin cells. Both the setup and the principle of this high precision measurement system have been previously introduced in detail<sup>1</sup>. The coin cells were placed in an oven with temperature set at 30°C for the entire experiment, while a high precision source meter (Keithley 2401) was used

to charge/discharge the cells to a specific potential (ranging from 3.4 V to 4.9 V) and subsequently to measure the leakage current. During the measurement, the working electrode was held at a specific potential using the source meter to realize an equilibrium in the electrochemical double layer on the surface of working electrode. In this case, the electron went through external circuit, which was monitored by Keithley 2401, can be ascribed to oxidation of the solvent at the surface of the working electrode. Since the leakage current measured here is basically proportional to the rate of the charge transfer reaction between the working electrode and the electrolyte, it can be used as an indicator of the reaction rate of the side reactions quantitatively.

In a typical measurement, the Al/Li cell was charged to 3.4 V with a current of 0.0334 mA. And then, after being held at that potential for 10 hours, the cell was charged to a higher potential at constant voltage with a limit current of 0.3 mA. The typical current relaxation collected during 10 hours of potentiostatic polarization was shown in Figure S1 in black line. In order to alleviate the impact of the high frequency noise and to get rid of the potential impact of slow electrochemical double layer charging, an exponential decay function (red line in Figure S1) with a formula of  $y = A_1 \cdot \exp(-x/t_1) + y_0$  was used to extract the static leakage current,  $y_0$  in the equation. Therefore, in Figure S1, the leakage current  $y_0$  was 0.03116  $\mu\text{A}$  with a standard error of 9.08674E-4.

*X-ray photoelectron spectroscopy (XPS) analysis* - XPS measurements were performed with a Physical Electronics Quantera Scanning X-ray Microprobe. This system uses a focused monochromatic Al K $\alpha$  X-ray (1486.7 eV) source for excitation and a spherical section analyzer. The instrument has a 32-element multichannel detection system. The X-

ray beam is incident normal to the sample and the photoelectron detector is at 45° off-normal. High energy resolution spectra were collected using a pass-energy of 69.0 eV with a step size of 0.125 eV. For the Ag 3d<sub>5/2</sub> line, these conditions produced a FWHM of 1.07 eV. The binding energy (BE) scale is calibrated using the Cu2p<sub>3/2</sub> feature at 932.62 ± 0.05 eV and Au 4f<sub>7/2</sub> at 83.96 ± 0.05 eV. XPS depth profile was obtained by bombarding the surface of Al using 2 kV Ar<sup>+</sup> ions and the raster size was 3mm× 3mm. The calibrated sputtering rate was 4.7 nm/min using known thickness SiO<sub>2</sub>/Si referenced materials.

*Density functional theory calculations* - All energy calculations and small molecule geometry optimizations were performed at the B3LYP/6-311++g(d) level of theory with G09 software<sup>2</sup>. This level of theory was employed previously in ethylene carbonate oxidation studies<sup>3</sup>. We have employed polarized continuum model to include solvation effects using value of static dielectric constant of 89.78, corresponding to ethylene carbonate at 40 °C<sup>4</sup>. Larger clusters for amorphous alumina derived from periodic structures<sup>5</sup> were partially optimized at B3LYP/6-31g\* level followed by single-point energy evaluations.

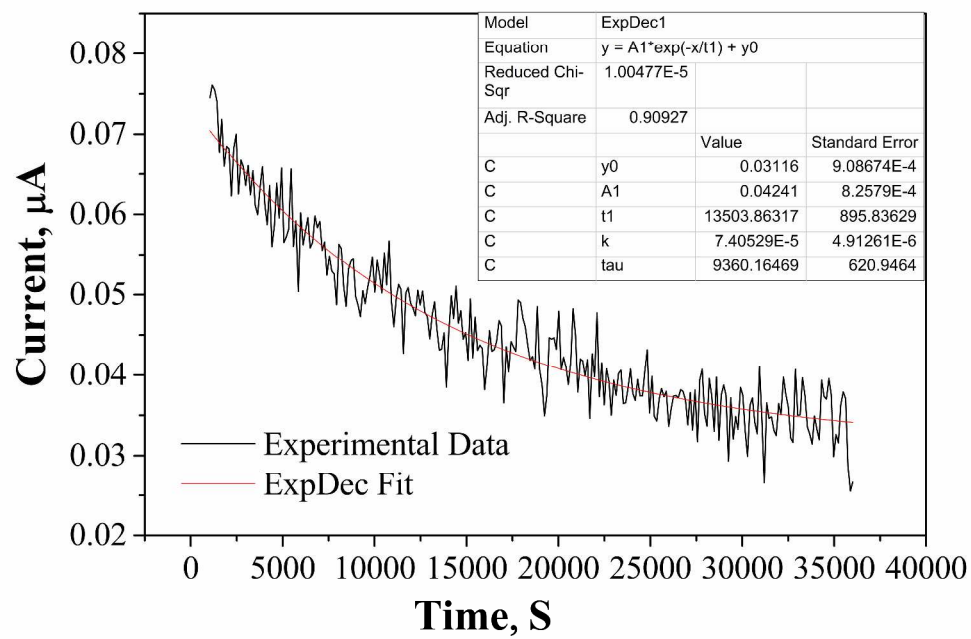


Figure S1 Typical decay of current being held at certain potential for 10 hours.

Table S1 Reaction energies and oxidation potentials of EC in the presence of different functional groups on alumina calculated using B3LYP functionals and PCM solvation model<sup>6-7</sup>.

Reaction	$\Delta G$ , eV	Eox, V <sup>a</sup>
$EC \rightarrow EC^+$		7.22, 7.01 <sup>b</sup>
$EC^+ \rightarrow EC(-H) + H^+$	0.5	7.72
$EC + EC^+ \rightarrow EC(-H) + ECH^+$	-1.28 <sup>b</sup>	5.94 <sup>b</sup>
$EC^+ + Al(OH)_3 \rightarrow EC(-H) + Al(OH)_2OH_2^+$	-1.41	5.82
$EC^+ + Al(OH)_4^- \rightarrow EC(-H) + Al(OH)_3OH_2$	-2.47	4.75
$EC^+ + Al(OH)_2SH \rightarrow EC(-H) + Al(OH)_2SH_2^+$	-0.95	6.28
$EC^+ + Al(OH)_3SH^- \rightarrow EC(-H) + Al(OH)_3SH_2$	-2.03	5.21
$EC^+ + Alumina^c \rightarrow EC(-H) + [Alumina1H]^+$	-1.78	5.44
$EC^+ + Alumina^c \rightarrow EC(-H) + [Alumina2H]^+$	-1.59	5.20

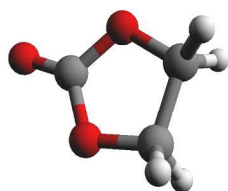
<sup>a</sup>Oxidation potentials relative to Li/Li<sup>+</sup> reference electrode starting with neutral EC on the left side of the reaction.

<sup>b</sup>From ref. [L.Xing and O. Borodin<sup>3</sup>]

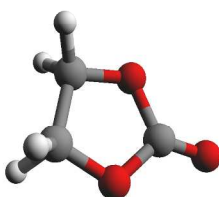
<sup>c</sup>For alumina models (Alumina, Alumina1H and Alumina2H) represented by clusters derived from a periodic model of amorphous alumina, see Fig. S1.



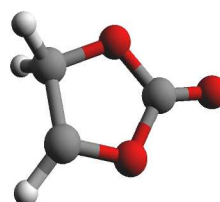
Ethylene Carbonate (EC)



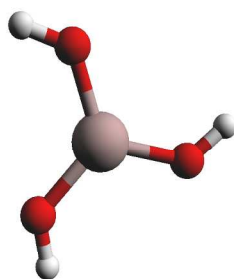
EC+



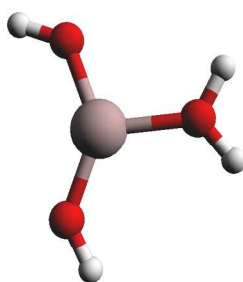
EC(-H)



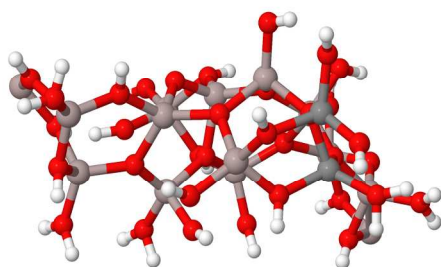
Al(OH)<sub>3</sub>



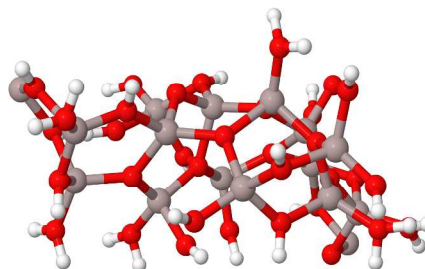
Al(OH)<sub>2</sub>OH<sub>2</sub><sup>+</sup>



Alumina



Alumina1H



Alumina2H

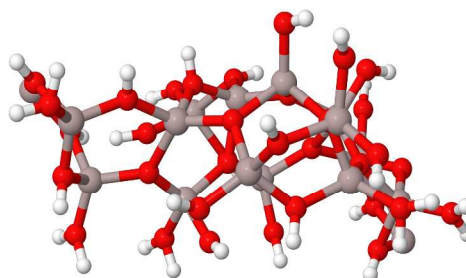


Figure S2 Structure of EC at different state, alumina models (Alumina, Alumina1H and Alumina2H) represented by clusters derived from a periodic model of amorphous alumina

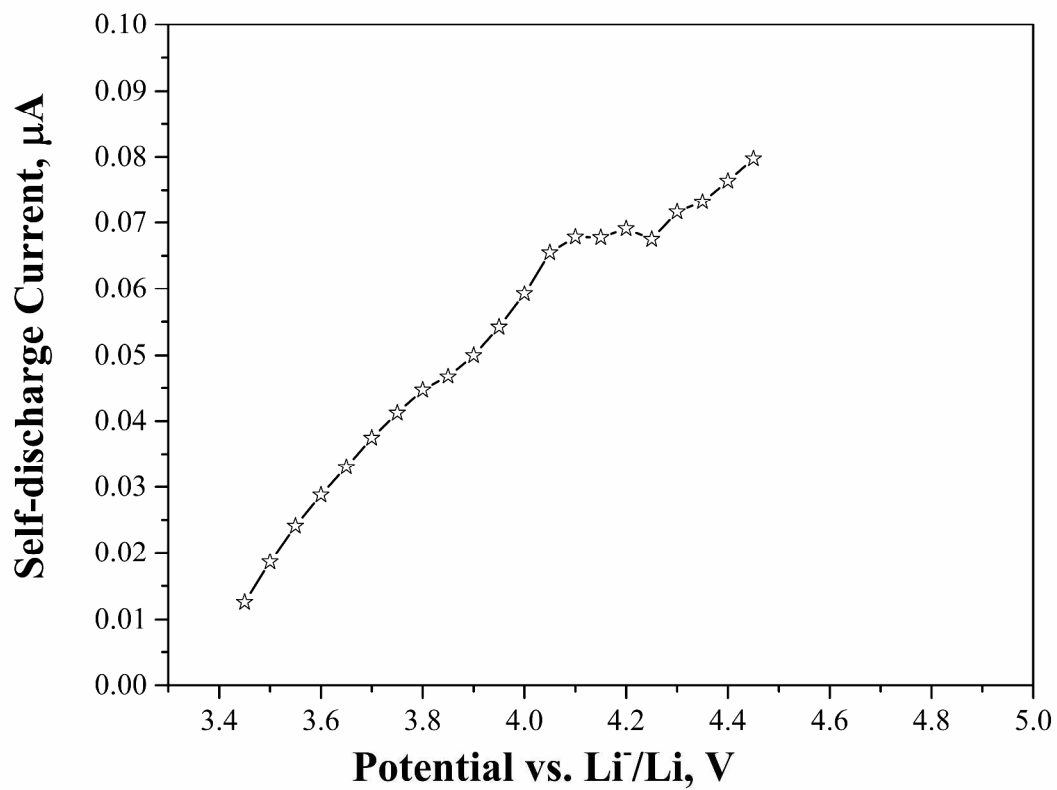


Figure S3 Potential-dependent of the static parasitic current for conditioned aluminum foil by repeated cycling between 3.4 V and 4.8 V for 5 cycles. The electrolyte used was 1.2 M  $\text{LiPF}_6$  in EC/EMC (3:7 by weight).

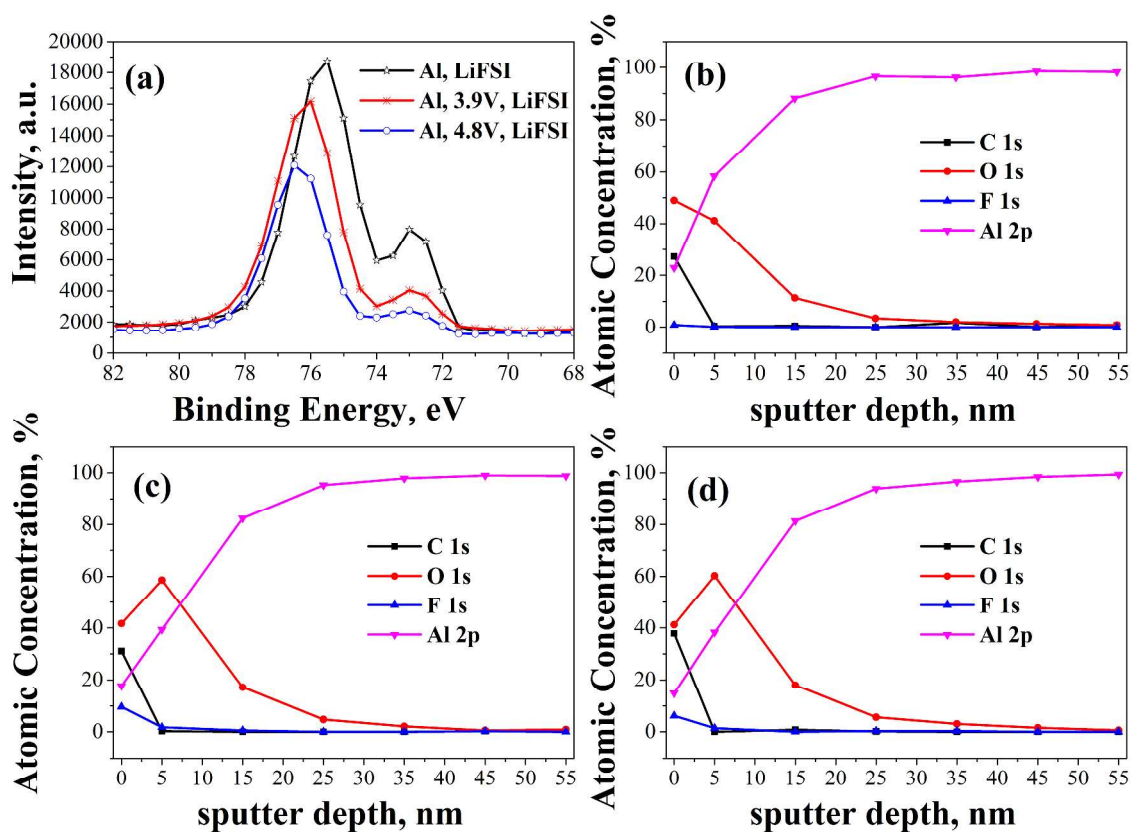


Figure S4 (a) XPS profiles of aluminum foils before and after the anodic treatment in 1.2 M LiFSI in EC/EMC (3:7 by weight); XPS depth profile analysis of aluminum foils (b) bare Al foil, (c) being anodic treated at 3.9 V, and (d) being anodic treated at 4.8 V.

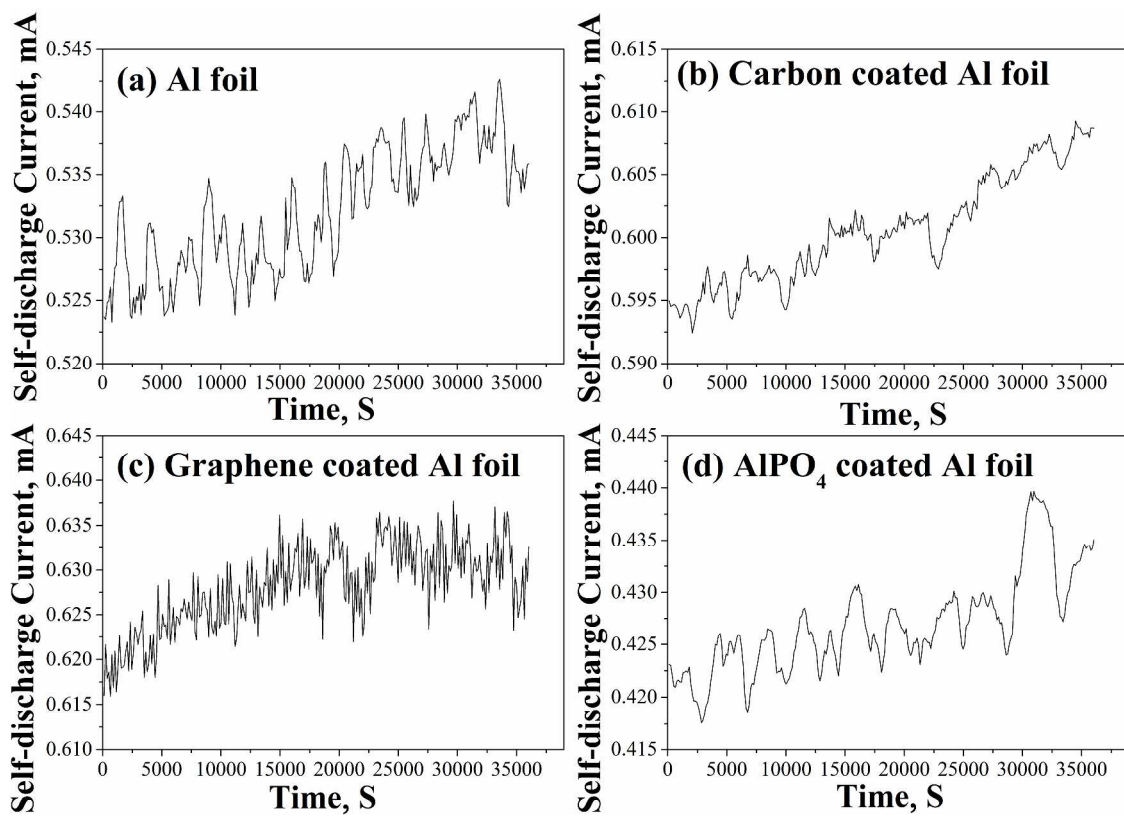


Figure S5 Decay of current for (a) Al, (b) carbon coated Al, (c) graphene coated Al, and (d)  $\text{AlPO}_4$  coated Al in LiFSI based electrolyte at 4.2 V.

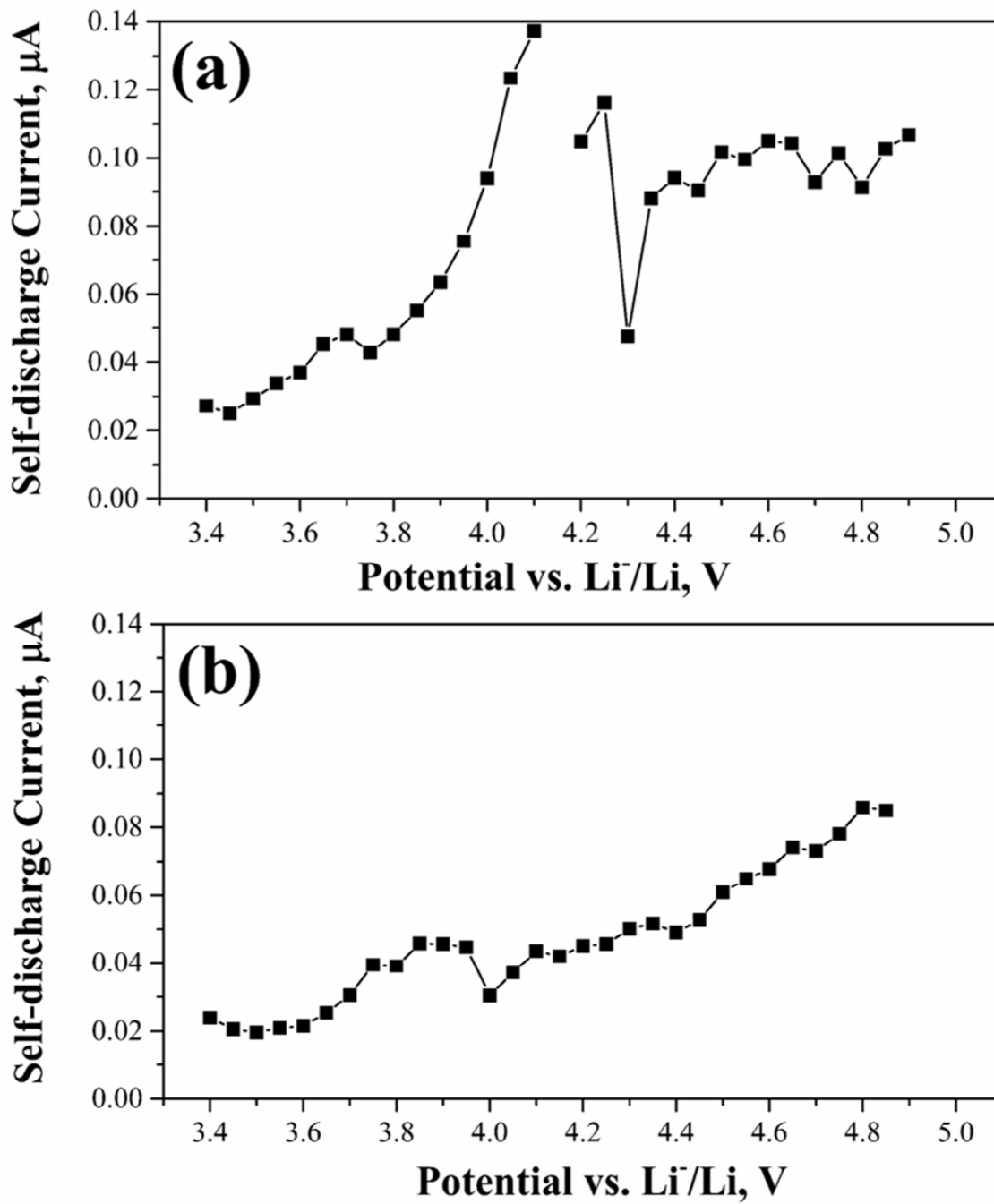


Figure S6 Potential-dependent of the static parasitic current for aluminum foil in (a) 1.2 M  $\text{LiPF}_6$  in FEC/EMC (3:7 by volume), (b) 1.2 M  $\text{LiPF}_6$  in mixture solvent of FEC and fluorinated ether (3:7, by weight).

- (1) Zeng, X. Q.; Xu, G. L.; Li, Y.; Luo, X. Y.; Maglia, F.; Bauer, C.; Lux, S. F.; Paschos, O.; Kim, S. J.; Lamp, P.; et al. Kinetic Study of Parasitic Reactions in Lithium-Ion Batteries: A Case Study on  $\text{LiNi}_{0.6}\text{Mn}_{0.2}\text{Co}_{0.2}\text{O}_2$ . *Acs Appl. Mater. Inter.* **2016**, *8*, 3446-3451.
- (2) Frisch, M. J.; Trucks, G. W.; Schlegel, H. B.; Scuseria, G. E.; Robb, M. A.; Cheeseman, J. R.; Scalmani, G.; Barone, V.; Mennucci, B.; Petersson, G. A.; et al. *Gaussian 09*, Gaussian, Inc, 2009.
- (3) Xing, L. D.; Borodin, O. Oxidation Induced Decomposition of Ethylene Carbonate from DFT Calculations - Importance of Explicitly Treating Surrounding Solvent. *Phys. Chem. Chem. Phys.* **2012**, *14*, 12838-12843.
- (4) Payne, R.; Theodorou, I. E. Dielectric Properties and Relaxation in Ethylene Carbonate and Propylene Carbonate,. *J. Phys. Chem.* **1972**, *76*, 2892-2900.
- (5) Adiga, S. P.; Zapol, P.; Curtiss, L. A. Structure and Morphology of Hydroxylated Amorphous Alumina Surfaces. *J. Phys. Chem. C* **2007**, *111*, 7422-7429.
- (6) Cossi, M.; Rega, N.; Scalmani, G.; Barone, V. Energies, Structures, and Electronic Properties of Molecules in Solution with the C-PCM Solvation Model. *J. Comput. Chem.* **2002**, *24*, 669-681.
- (7) Tomasi, J.; Mennucci, B.; Cammi, R. Quantum Mechanical Continuum Solvation Models. *Chem. Rev.* **2005**, *105*, 2999-3093.